

Chemically cross-linked poly(vinyl alcohol) electrospun fibrous mats as wound dressing materials

Berta Díez,^a W Joseph A Homer,^b Laura J Leslie,^b Georgios Kyriakou,^c Roberto Rosal,^a Paul D Topham^b and Eirini Theodosiou^{b*} 



Abstract

BACKGROUND: Poly(vinyl alcohol) (PVA) is a synthetic biocompatible polymer that is extensively used by the medical and pharmaceutical industries due to its FDA approval for *in vivo* applications. Its highly hydrophilic nature makes it an ideal wound dressing material, especially in the form of nanofibrous mats.

RESULTS: In this work, electrospun PVA-based scaffolds suitable for wound management were created. Chemical cross-linking with citric acid and glyoxal was employed to enhance the supports' stability in aqueous environments, and cellulose nanocrystals were added during the electrospinning process to improve the mechanical properties of the final constructs. Varying the concentrations of the cross-linking agents (0.12–1 wt% citric acid and 0.06–0.5 wt% glyoxal), allowed the control of the rate and extend of dissolution, thereby tuning the properties of the materials to the specific wound types (e.g. acute vs chronic). There was an inverse relationship between the amount of cross-linkers used and the mats' weight loss (ranging from 2% to 18%) after 6 days immersion in water. All supports sustained the growth of human fibroblasts (>85% viability), whereas there was no biofilm formation when in contact with *S. aureus* for 24 hours. The presence of cellulose nanocrystals did not affect cytocompatibility but improved the mechanical properties of the non-woven fibres.

CONCLUSION: Tailor-made biocompatible electrospun mats showing antimicrobial behaviour were successfully created through altering the concentration of chemical cross-linkers. This flexible approach offers the potential of matching the dressing to the wound type and offering a more targeted solution to wound management.

© 2021 Society of Chemical Industry (SCI).

Supporting information may be found in the online version of this article.

Keywords: biocompatible polymers; nanocellulose; wound management; antimicrobial

INTRODUCTION

Hydrogels are cross-linked polymeric networks able to absorb large quantities of water or biological fluids. Their high water-holding capacity, soft consistency, and excellent biocompatibility make them an ideal class of materials to use in clinical devices.^{1,2} Hydrogels can be produced in different forms, such as membranes, foams, films, and fibres. Out of these, the ever-increasing popularity of hydrogel-based nanofibers as scaffolds for wound management can be attributed to a combination of properties that promote the wound-healing process. These properties include: high surface area to volume ratio (which favours the adhesion of cells within the hydrogel network), and increased porosity and interconnectivity within the polymeric network, which enhances oxygen and water permeability (thereby allowing cell respiration and maintaining the moist wound environment required to prevent cell dehydration), as well as efficient absorption of excess exudates. In fact, the morphology of nanofibrous materials closely mimics the natural environment of the extracellular matrix, thereby, creating a favourable milieu for cell growth.^{3–6}

Although different techniques can be employed for the creation of micro- and nano-fibres,⁷ electrospinning seems to be the method of choice for most applications because it is simple, fast, scalable, cost-effective, and can be used with a variety of natural and synthetic polymers.^{8–10}

Poly(vinyl alcohol) (PVA) is a synthetic hydrophilic linear polymer that has been used extensively in the biomedical field due to its biocompatibility, biodegradability, and lack of toxicity.^{4,11,12} PVA is highly soluble in water due to the large number of hydroxyl groups that interact with the water molecules through hydrogen bonds; therefore, its water stability needs to be

* Correspondence to: E Theodosiou, Aston Institute of Materials Research, Aston University, Aston Triangle, Birmingham B4 7ET, UK, E-mail: e.theodosiou@aston.ac.uk

a Department of Analytical Chemistry, Physical Chemistry and Chemical Engineering, University of Alcalá, Madrid, Spain

b Aston Institute of Materials Research, Aston University, Birmingham, UK

c Department of Chemical Engineering, University of Patras, Patras, Greece

improved before it can be used in aqueous environments. Several strategies have been proposed for PVA-based nanofibers, including physical cross-linking (such as ionic interactions, crystallization, and hydrogen bonding) and chemical cross-linking (such as copolymerization, chemical reaction, and high energy irradiation).^{13–15} Chemical cross-linking provides stable covalent bonds between the polymer chains, thereby improving the mechanical properties of the support and creating a water-insoluble hydrogel.^{16,17} The reagents normally used for chemical cross-linking include polycarboxylic acids, such as 1,2,3,4-butanetetracarboxylic acid (BTCA) or citric acid (CA), and some aldehydes, such as glutaraldehyde, formaldehyde or glyoxal,^{18–20} all of which can interact with the hydroxyl groups present in the PVA through the formation of esters (with the polycarboxylic acids) or acetyl bonds (with the aldehydes).^{21,22}

In this work, we produced biocompatible electrospun scaffolds to be used as part of wound dressing materials. Citric acid, a natural tricarboxylic acid present in citrus fruits, was used as a cross-linking agent because of its ability to counterbalance the hydrophilicity of PVA.^{16,19} Glyoxal, the simplest of the dialdehydes, was also selected to reinforce the cross-linking interaction between the polymeric chains. Although glyoxal is not as widely used as glutaraldehyde for the cross-linking of biomaterials, it is considered much safer when in contact with human cells and, therefore, it is finding increasing applications in areas such as bone regeneration.²³ By changing the concentrations of these cross-linking agents, we are able to tune the rate and extend of dissolution of the scaffolds to suit the final application. For example, the healing process of acute wounds (e.g., those that heal after an average of 3 weeks) is much shorter than that of chronic ones (e.g., those that show no reduction in size after 2–4 weeks); therefore, the 'one size fits all' wound dressing approach will not produce a desirable therapeutic effect.^{24,25} Additionally, to further improve the mechanical characteristics of the scaffolds, cellulose nanocrystals (CNC) were incorporated during the electrospinning process. Nanocellulose is a natural, hydrophilic, biodegradable, and non-toxic polymer that has been used extensively as reinforcing filler in biotechnology and biomedicine due to its excellent mechanical strength and the properties it can infer as a key component of a composite material.^{26–28}

Following their production, our cross-linked electrospun mats were assessed in terms of fibre morphology, chemical composition, mechanical properties, swelling and degradation behaviour, antimicrobial effect against *Staphylococcus aureus* (a common pathogen involved in wound infections), and cytotoxicity to human fibroblast cells.

MATERIALS AND METHODS

Materials

Poly(vinyl alcohol) (PVA, Mowiol 18–88, MW 130 kDa, 88% hydrolysed); citric acid (CA, 99%); glyoxal (40% wt in H₂O); glutaraldehyde solution (25% in H₂O); Triton X-100; trypsin-EDTA (ethylenediamine tetraacetic acid) solution (10x); MTT (3-(4,5-dimethylthiazol-2-yl)-2, 5-diphenyltetrazolium bromide); Dulbecco's Modified Eagle's Medium (DMEM); Fetal Bovine Serum (FBS, γ -irradiated, sterile filtered); L-glutamine (PharmaGrade); antibiotic antimycotic solution (100x); and MEM non-essential amino acid solution (100x) were purchased from Sigma-Aldrich Company Ltd (Gillingham, UK). Hoechst dye solution 33 342 (Trihydrochloride, Trihydrate; Invitrogen), ActinGreen

Table 1. Composition of the 14% (w/v) PVA solutions prior to electrospinning

Electrospun Mat	Citric acid (% w/w)	Glyoxal (% w/w)	Cellulose nanocrystals (% w/w)
PVA(C)	-	-	-
PVA(H) ^a	-	-	-
PVA(1)	1	0.5	-
PVA(1)/CNC(1)	1	0.5	1
PVA(1)/CNC(2)	1	0.5	2
PVA(2)	0.5	0.25	-
PVA(3)	0.25	0.12	-
PVA(4)	0.12	0.06	-

^a Sample PVA(H) is the physically cross-linked (heated at 180 °C for 30 min) version of the control PVA(C) post-electrospinning.

488 (ReadyProbes Reagent; Invitrogen), and FilmTracer FM 1–43 Green Cell stain (Invitrogen) were acquired from Thermo Fisher Scientific (Waltham, MA, USA). All other materials not identified above were obtained from Sigma-Aldrich Company Ltd and Thermo Fisher Scientific. The cellulose nanocrystals CelluForce NCC[®] (nominal average length and diameter of 150 nm and 7.5 nm, respectively) originated from wood pulp and were purchased from CelluForce (Montreal, Canada). Human skin fibroblasts (cell line 142BR) were obtained from ECACC (European Collection of Authenticated Cell Cultures, Porton Down, UK). *Staphylococcus aureus* (CETC 240, strain designation ATCC 6538P) was acquired from LGC Standards (Teddington, UK).

Preparation of electrospun fibres

PVA 14% (w/v) was dissolved in distilled water under stirring at room temperature. For samples PVA(1)–(4), the cross-linking agents (citric acid and glyoxal) were directly added into the polymer solution (Table 1 lists the concentrations used), heated at 80 °C for 1 h under continuous stirring, and subsequently cooled down to room temperature. For PVA(1)/CNC(1) and PVA(1)/CNC(2), the corresponding amount of cellulose nanocrystals was added to the PVA solution to obtain final concentrations of 1% and 2% (w/w), respectively, and the suspensions were kept under continuous stirring for 24 h. After this time, the cross-linking agents were added as described above.

All samples were degassed and transferred to a 5 mL standard syringe fitted with a 22G blunt stainless-steel needle using a precision/syringe pump (NE-300, New Era Pump Systems Inc., USA) at a flow rate of 0.6 mL h⁻¹. A high voltage of 22 kV was applied (Simco, MP Series CM5 30 P, Charging Generator Output 22 kV DC), and the fibres were collected on a grounded stainless-steel plate covered with aluminium foil and positioned 15 cm away from the tip of the needle. Each sample was electrospun for 2 h at ~20 °C ambient temperature and RH30%. Following electrospinning, the crystallinity of the sample identified as PVA(H) (Table 1) was increased by heating at 180 °C (Fan Assisted High Temperature Oven 80 HT, SciQuip Ltd, Wem, UK) for 30 min. The rest of the samples were heated at 125 °C for 24 h to ensure water evaporation and, in the case of PVA(1)–(4) and PVA (1)/CNC (1)–(2), to ensure the completion of the chemical cross-linking reaction. A scheme of the reactions involved is presented in Fig. S1.

Characterization of electrospun mats

The morphology of the electrospun fibres was studied using a Zeiss DSM-950 Scanning Electron Microscope (Zeiss, Oberkochen, Germany) operated at 25 kV. Prior to observation, each sample was sputter coated with gold. Fibre diameters were measured using Image J software (National Institutes of Health, Bethesda, MD, USA) and reported as an average value of 35 independent measurements. Fourier transform infrared spectroscopy analyses were carried out using a PerkinElmer Frontier™ FT-IR spectrometer (PerkinElmer Inc., Waltham, MA, USA). FT-IR spectra were recorded in the attenuated total reflection (ATR) mode, over the 4000–700 cm^{-1} range with a resolution of 4 cm^{-1} within 64 scans.

The mechanical properties of the non-woven fibrous mats (10 × 50 mm; 250 μm average thickness; $n = 3$) were measured by means of uniaxial tensile tests using a universal uniaxial tensile testing machine (Electroforce® 3230; TA Instruments, MN, USA) at a rate of 10 mm min^{-1} with samples taken to failure. Stress–strain curves were obtained and mean averages of the ultimate tensile strength (UTS), Young's Modulus (E), and elongation at break were calculated.

The crystallinity of the samples was evaluated by means of wide-angle powder X-ray diffraction (XRD) on a Bruker D8 Advance diffractometer equipped with a LynxeyePSD detector and with $\text{Cu K}\alpha_{1,2}$ radiation (40 kV and 40 mA, 0.02 mm Ni K β absorber, 10–80° 2θ range, a step scan of 0.02°).

Water uptake and weight loss profiles were determined by soaking 15 mm diameter disks of the different specimens in 5 mL distilled water at room temperature for 1, 3, and 6 days. The dry weight of the discs was measured after water immersion and subsequent drying at room temperature to constant weight. The weight of water-swollen membranes was recorded immediately after removing the excess surface water using a filter paper. The swelling ratio and weight loss were calculated using Eqns (1) and (2):

$$\text{Swelling ratio (\%)} = \frac{W_s - W_d}{W_d} \times 100 \quad (1)$$

$$\text{Weight loss (\%)} = \frac{W_0 - W_d}{W_0} \times 100 \quad (2)$$

where: W_0 is the initial weight of the sample; W_s is the weight of water-swollen samples; and W_d is the dry weight after water immersion.

Cell culture

Human skin fibroblasts were grown in cell culture flasks containing Dulbecco's Modified Eagle's Medium supplemented with 10% FBS, 1% L-glutamine, 1% antibiotic antimycotic solution (100x), and 1% non-essential amino acid solution (100x). Cells were grown to up to 80% confluence in a Heracell 150i CO_2 incubator (Thermo Scientific, Fisher Scientific, Waltham, MA, USA) in a controlled environment (5% CO_2 ; 37 °C) prior to initiating the assays.

Cytotoxicity and cell viability

Cytotoxicity was assessed following ISO standard 10993–5:2009.^{29,30} The cytotoxic response was evaluated by two different tests, namely, direct contact (to study the effect of the direct physical interaction between cells and electrospun mats), and extract test (aiming to investigate the interaction between leachable by-products and the cells). A schematic representation of

both assays is shown in Fig. S2. Cells cultured in the absence of electrospun mats were used as a blank or negative control (C-), and the addition of 70% (v/v) ethanol was used as a positive cytotoxic response (C+).

For both tests, cells were seeded in sterile 96-well microtiter plates at a concentration of 5×10^3 cells per well and incubated at 37 °C and 5% CO_2 . Once a cell monolayer was formed, and in the case of the direct contact test, the mats were placed on top of the cells and left to incubate for 24 and 72 h. After incubation, the mats and medium were removed using a sterile pipette connected to a vacuum line to avoid potential damage to the cell monolayer. For the extract test, electrospun mats (1.4 $\text{cm}^2 \text{mL}^{-1}$) were added to Eppendorf tubes (Eppendorf UK Ltd, Stevenage, UK) containing culture medium and left for 24 and 72 h with constant shaking at 100 rpm (Orbital Shaker GFL-3005, DD Biolab S.L., Barcelona, Spain). Following monolayer formation, the cell growth medium was replaced by the extraction liquid and incubated for another 24 h.

Cell viability after both tests was assessed by the MTT colorimetric assay, which is based on the principle that metabolically active cells are able to transform the yellow-coloured tetrazolium salt into the purple-coloured formazan.³¹ MTT (20 μL of a 50 mg mL^{-1} solution in PBS) was added to the culture medium and incubated at 37 °C and 5% CO_2 . After 4 h, the medium was removed and the precipitated purple formazan was dissolved in 100 μL DMSO. The product was quantified by absorbance readings at 570 nm using a universal microplate reader ELx800™ (BioTek Instruments, Winooski, VT, USA).

Cell morphology and proliferation

The growth and proliferation of fibroblasts on the surface of the mats was visualized using confocal microscopy. Fibroblast cells (1.5×10^4 cells) were added to the microtiter plate wells containing electrospun mats and incubated at 37 °C and 5% CO_2 for 24 and 72 h. Each scaffold was subsequently washed with PBS, fixed using 2.5% glutaraldehyde solution for 30 min, washed with PBS, permeabilized with 0.1% Triton X-100 for 10 min, and washed again with PBS. F-Actin filaments were stained using ActinGreen 488 reagent and cell nuclei using Hoechst 33342 dye, both according to the manufacturer's instructions. Cells were visualised at 485/518 nm (excitation/emission for ActinGreen 488) and 353/483 nm (excitation/emission for Hoechst 33342) using a fluorescent microscope (Leica TCS SP5, Leica Microsystems, Wetzlar, Germany).

To identify any morphological changes resulting from the contact between the fibroblast cells and the electrospun mats, at the end of the 72 h incubation period, cells were fixed using 2.5% glutaraldehyde solution, washed with PBS, and observed with an optical microscope (Eclipse E200-LED, Nikon Corporation, Melville, NY, USA) (x10 magnification).

Antimicrobial behaviour

The microorganism used in these studies was *Staphylococcus aureus*, a gram-positive bacterium that is the main cause of superficial infections in wounds. Bacterial cultures (kept at –80 °C) were reactivated using nutrient broth (NB) culture medium (peptone 10 g L^{-1} , sodium chloride 5 g L^{-1} , meat extract 5 g L^{-1}) at pH 7.0 and 36 °C under constant agitation (250 rpm). Cell growth was monitored by measuring optical density (OD) at 600 nm (Shimadzu UV-1800, Shimadzu Europa GmbH, Duisburg, German) until the cells reached stationary phase. The antimicrobial behaviour of the PVA mats was tested using the colony counting unit

(CFU) assay. For that, the mats were placed in sterile 24-well microtiter plates and exposed to an initial bacterial culture of 10^6 cells mL^{-1} at 36 °C. After 24 h of incubation, the mats were carefully removed, washed with sterile distilled water, and incubated in a soybean-casein-digest-lecithin-polyoxyethylene sorbitan monooleate (SCDLP broth) for 30 min at room temperature with continuous shaking to achieve efficient recovery of the bacteria from the mat surface in accordance with the ISO 22196 protocol.

The liquid medium was subsequently recovered and diluted 10-fold with PBS using serial dilutions. Ten microlitres from each dilution was spot-plated on solid agar and then counted following 20 h incubation at 36 °C. The counting was performed in triplicate.

Bacterial colonization was visualised using the FilmTracer FM 1–43 Green Cell stain according to the manufacturer's instructions. Biofilm formation was observed by fluorescent microscopy (Leica TCS SP5, Leica Microsystems, Wetzlar, Germany) at

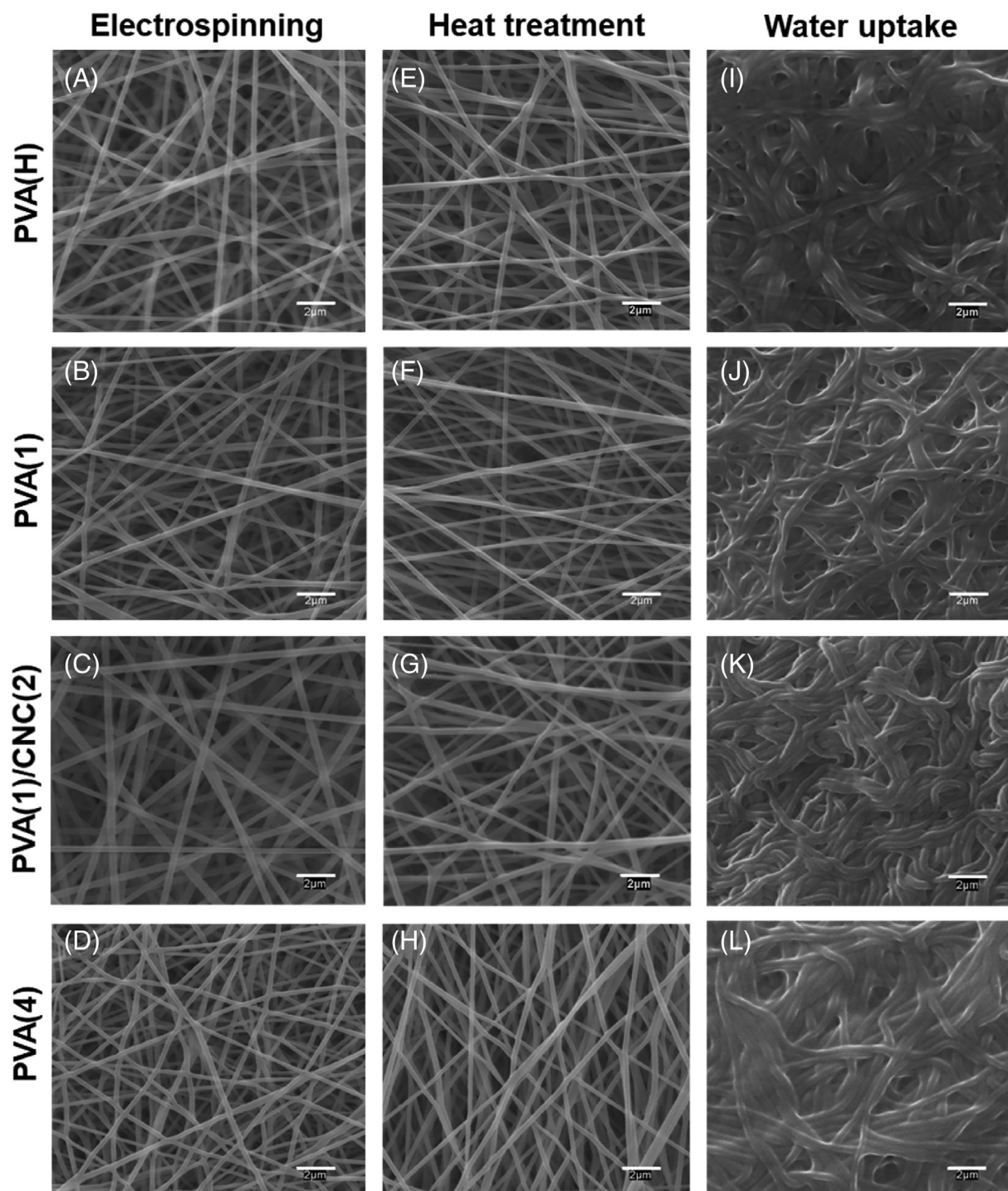


Figure 1. SEM images (magnification 5000x) of PVA(H), PVA(1), PVA(1)/CNC(2), and PVA(4) mats: immediately after electrospinning (A–D); after heat treatment (E–H); and after water uptake for 24 h (I–L). The composition of the mats can be found in Table 1. PVA(H) was heat treated at 180 °C for 30 min, and PVA(1), PVA(1)/CNC(2), and PVA(4) were heat treated at 125 °C for 24 h. Scale bars: 2 μm .

excitation/emission 472/580 nm, as well as by SEM images. For the latter, the mats were inoculated with 10^6 cells/mL of *S. aureus*. After 24 h of incubation at 36 °C, the mats were rinsed with distilled water, fixed using 5% glutaraldehyde, and dehydrated with ethanol (25–50–70–90–100%) and acetone (100%) prior to visualization with a Zeiss DSM-950 Scanning Electron Microscope (Zeiss, Oberkochen, Germany).

RESULTS AND DISCUSSION

In this study, a series of fibrous mats based on high molecular weight PVA (130 kDa; 88% hydrolysed) was prepared using needle-based electrospinning (for 2 h at 0.6 mL h⁻¹ flow rate, 22 kV and 15 cm tip to collector distance). The resulting mats were cross-linked, either chemically (using different concentrations of glyoxal and citric acid) or physically (using heating at 180 °C for 30 min). Furthermore, CNC (1% and 2% w/w) were incorporated to the PVA(1) mats (*i.e.*, those with the highest concentration of chemical cross-linkers and, therefore, the best water stability) to improve the mechanical strength of the final constructs.

Morphological and chemical characterization of PVA electrospun mats

Figure 1 shows SEM images of PVA(H), PVA(1), PVA(1)/CNC(2), and PVA(4) electrospun mats (Table 1 shows their compositions) as representatives of physical cross-linking, highest concentration of chemical cross-linkers, highest percentage of CNC in the sample, and lowest concentrations of chemical cross-linkers, respectively. Images of PVA(1)/CNC(1), PVA(2), and PVA(3) are shown in Fig. S3.

In all cases, a clear structure of homogenous and interconnected nanofibers, free from defects, can be observed. Furthermore, the mats maintain their structure following heating and after being immersed in water for 24 h. Although CNCs are not visible in the SEM images (Fig. 1(C), (G) and (K)), other techniques (refer to Figure 5 and Table 4) verify their presence, suggesting that they are well-distributed within the fibres.

Fibre diameter was measured from the SEM images, and the results are presented in Table 2. There is a small decrease in fibre diameter for all mats following chemical cross-linking and heat treatment. This agrees with the findings of Çay and co-workers, who reported that the incorporation of polycarboxylic acids, such as citric acid, increased the electrical conductivity of the electrospinning solution and produced thinner nanofibers compared to the controls.²¹

Following water immersion, the electrospun mats absorbed large amounts of water (400–800% swelling ratio), leading to an increase in fibre diameter, but the mats still retained their fibrous morphology, where the cross-links prevent dissolution or fragmentation of the fibres. As can be seen from Fig. 2, water uptake occurred within the first 24 h of immersion; afterwards, this water uptake was almost fully maintained (within experimental error) over the next 5 days for all chemically cross-linked samples. For the polymers that were heated without chemical cross-linker (PVA(H)), a slight decrease in swelling could be observed, whereas the control polymer that had no treatment (PVA(C)) dissolved almost immediately (and therefore does not feature in Fig. 2). This is due to the highly hydrophilic character of PVA that emerged as a result of the hydroxyl groups present in its repeating units.¹² Moreover, the swelling capacity of the mats decreased with increasing cross-linker loading. An increased degree of cross-

Table 2. Fiber diameter of electrospun mats immediately after electrospinning and following heating and water treatments. Data are represented as mean values for $n = 35 \pm 1$ standard deviation

Electrospun Mat	Fiber diameter (nm)		
	Untreated	Heat treated ^a	Water treated ^b
PVA(C)	303 ± 51	298 ± 47	– ^c
PVA(H)	302 ± 54	278 ± 35	381 ± 51
PVA(1)	280 ± 47	246 ± 32	367 ± 63
PVA(1)/CNC(1)	263 ± 35	232 ± 20	457 ± 48
PVA(1)/CNC(2)	258 ± 29	218 ± 14	523 ± 41
PVA(2)	254 ± 38	224 ± 27	396 ± 57
PVA(3)	256 ± 32	230 ± 31	453 ± 51
PVA(4)	245 ± 27	235 ± 27	559 ± 74

^a PVA(C), PVA(1)–(4) and PVA(1)/CNC(1–2) were heat treated at 125 °C for 24 h. PVA(H) was heat treated at 180 °C for 30 min.

^b Following 24 h of immersion in water.

^c Upon contact with water, the untreated mats dissolved immediately.

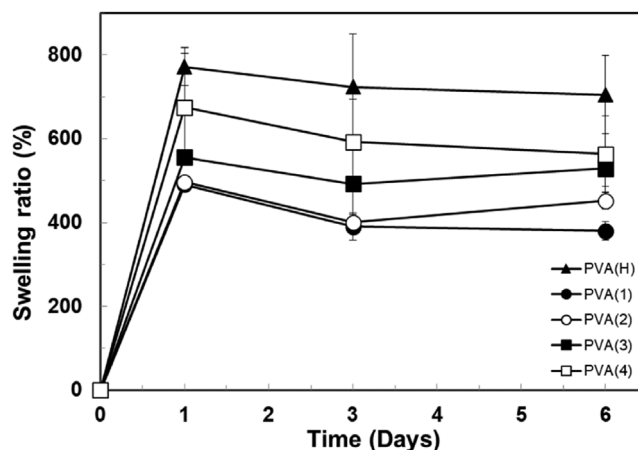


Figure 2. Swelling ratio profiles of PVA mats following immersion in DI water at room temperature.

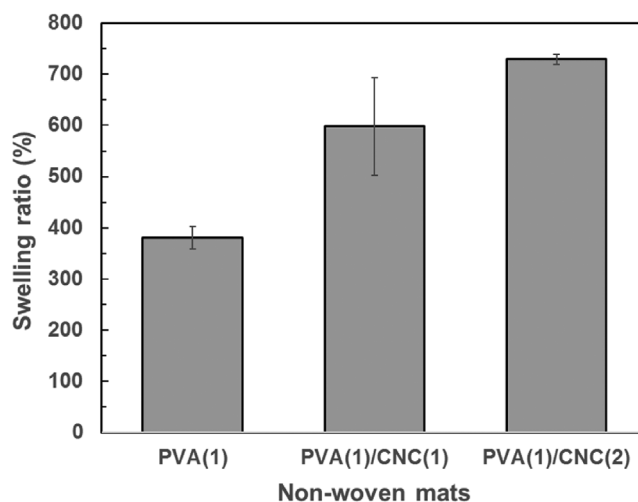


Figure 3. Swelling ratio profiles of PVA(1) pre and post incorporation of cellulose nanofibers, following immersion in DI water for 6 days at room temperature. Data show mean values for $n = 3 \pm 1$ standard deviation.

linking enhances the linkages between the polymer chains, leading to more rigid and less porous structures that are less prone to the diffusion of water molecules into their network.^{12,32,33}

The addition of CNC increased the ability of the mats to take up water (Table 2 and Fig. 3), and this is attributed to the abundance of hydroxyl groups on the CNC surface. During exposure to hydrogen bond-forming liquids (i.e., water), competitive hydrogen bonding disrupts the strong CNC-CNC and PVA-CNC interactions, leading to 'water responsive' materials.³⁴ The CNC incorporation to the PVA mats, therefore, enhances the hydrophilic nature of the supports and,

consequently, improves their ability to absorb water. The latter is a highly desirable property in wound management,^{25,28,35} where the presence of a moist milieu facilitates cellular and enzymatic activity, leading to accelerated angiogenesis, increased fibrinolysis, and successful healing.³⁶⁻³⁸

The chemical composition of the electrospun scaffolds was analysed by FT-IR and the spectra are presented in Fig. 4. The PVA mats exhibited a large adsorption band between 3200 and 3500 cm^{-1} that was attributed to O—H stretching. The absorption at 2850–3000 cm^{-1} corresponds to C—H stretching of alkyl

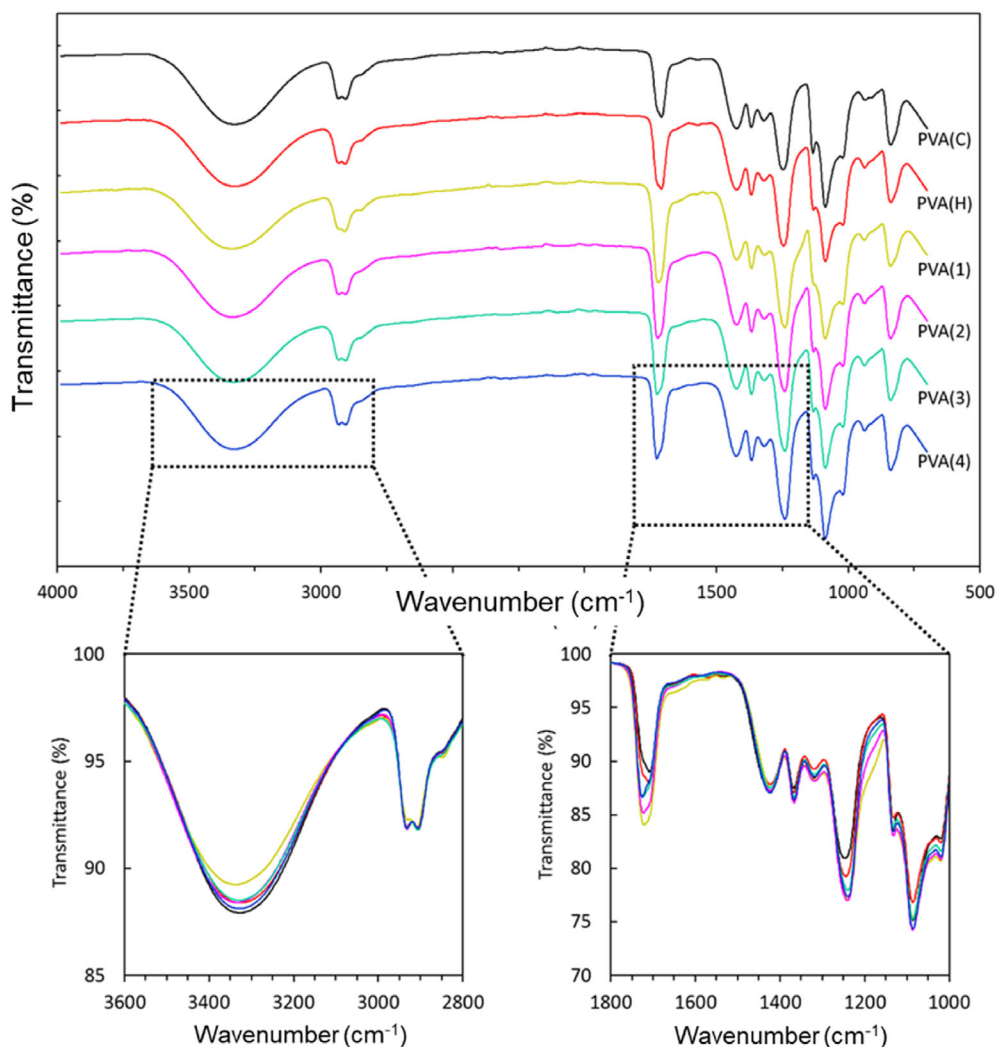


Figure 4. FT-IR spectra of the PVA(C), (H), and (1–4) electrospun mats prepared in this work (refer to Table 1 for composition of mats), with insets containing spectra normalized to the C—H stretch at 2910 cm^{-1} for examining transmission intensity changes around 3329 cm^{-1} , 1718 cm^{-1} , 1240 cm^{-1} , and 1100 cm^{-1} .

Table 3. Absorbance intensity ratios derived from FT-IR spectra, showing relative intensities between cross-linker associate bonds and native PVA hydroxyl bonds, normalized to the C—H stretch at 2910 cm^{-1}

Absorbance wavelength	Bond pair	PVA(C)	PVA(H)	PVA(1)	PVA(2)	PVA(3)	PVA(4)
1718/3329	C=O/O-H	0.90	1.03	1.45	1.23	1.09	1.02
1240/3329	C-O/O-H	1.50	1.71	2.11	1.96	1.90	1.89
1100/3329	C-O/O-H	2.01	1.97	2.27	2.20	2.12	2.12

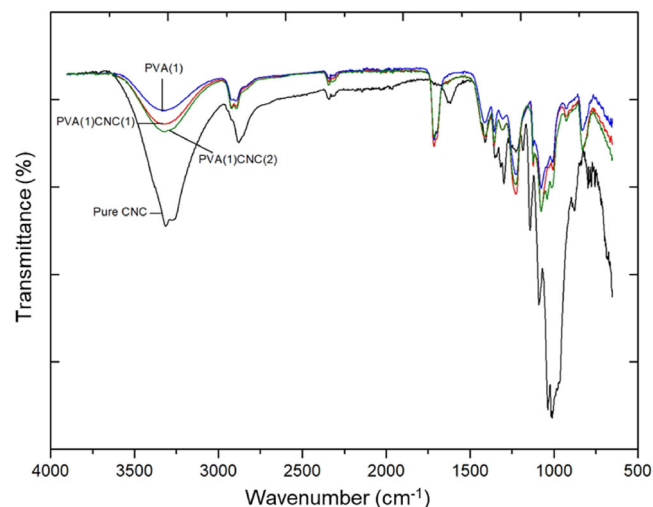


Figure 5. FT-IR spectra of the cellulose nanocrystal-loaded electrospun mats compared to pure cellulose nanocrystals and mats of equivalent composition without cellulose (refer to Table 1 for composition of mats), normalized to the O–H bending of pure CNC at 1638 cm^{-1} .

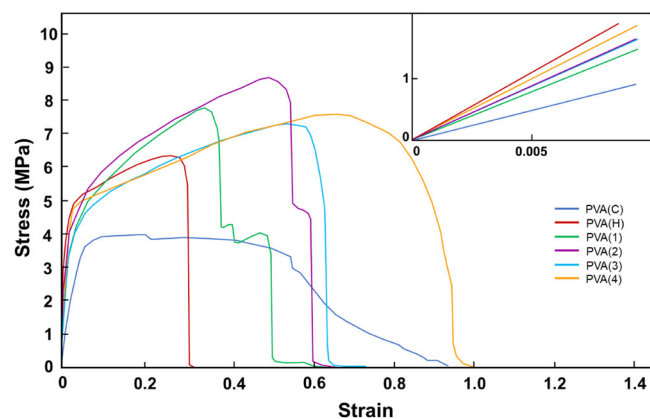


Figure 6. Representative stress–strain curves for the PVA electrospun mats. The inset shows an enlarged region of strain corresponding to the Young's moduli.

groups, while the peaks at 1680–1750 cm^{-1} are characteristic of C=O and C–O stretching that appeared after CA and glyoxal cross-linking, as well as from the remaining acetate groups in PVA following the saponification reaction of poly(vinyl acetate) during PVA production.³⁹

Chemical cross-linking of PVA was achieved by heat treatment at 125 °C for 24 h post electrospinning. After this time, the hydroxyl groups present in the PVA reacted with the carboxylic acid groups present in the citric acid through an esterification reaction and with the aldehyde groups present in the glyoxal through the formation of acetal bonds. The overlapping of FT-IR spectra displayed in the insets of Fig. 4 reveal a reduction in the bands located at 3200–3500 cm^{-1} , and an increase in band intensity at 1718 cm^{-1} upon addition of cross-linking agents, resulting in a change of absorbance intensity ratio (data normalized to the C–H stretch at 2910 cm^{-1}) from 0.9 for PVA(C) to 1.45 for PVA (1) that is attributed to the formation of ester carbonyl groups.²¹ The band at 1240 cm^{-1} , which is attributed to C–O stretching in ester bonds, also shows an increase in intensity relative to O–H stretching, and this is positively correlated with cross-linker

Table 4. Mean mechanical properties ± 1 standard deviation of the PVA electrospun mats prepared in this work ($n = 3$) to 1 decimal place

Electrospun Mat	Young's modulus (MPa)	UTS (MPa)	Elongation at break (%)
PVA(C)	75.9 \pm 9.5	3.5 \pm 0.7	54.2 \pm 11.8
PVA(H)	190.6 \pm 85.4	6.8 \pm 2.7	30.0 \pm 3.4
PVA(1)	124.4 \pm 27.8	6.4 \pm 0.8	32.8 \pm 14.7
PVA(1)/CNC(1)	156.3 \pm 33.2	9.6 \pm 1.2	51.0 \pm 6.4
PVA(1)/CNC(2)	185.4 \pm 30.2	14.9 \pm 0.9	49.0 \pm 4.4
PVA(2)	147.6 \pm 20.5	8.4 \pm 0.8	53.2 \pm 5.3
PVA(3)	158.0 \pm 33.0	7.7 \pm 0.6	60.0 \pm 5.8
PVA(4)	212.8 \pm 59.3	8.6 \pm 1.6	80.8 \pm 16.3

content, as shown in Table 3.⁴⁰ The table also shows a similar trend observed with the C–O stretching measured at 1100 cm^{-1} , with the increase being attributed to acetal bond formation following cross-linking with glyoxal.⁴¹ A summary of the absorption bands is provided in Table S1.

FT-IR analysis was used to confirm the presence of cellulose nanocrystals in the PVA nanofiber mats. Figure 5 shows collected spectra from PVA(1), CNC-loaded PVA mats, and pure cellulose nanocrystals. For both PVA(1)/CNC(1) and PVA(1)/CNC(2), there is an increased band intensity between 3100–3550 cm^{-1} that is characteristic of O–H stretching from the intermolecular and intramolecular hydrogen-bonded hydroxyl groups in cellulose. The band observed at 2901 cm^{-1} in the neat CNC spectrum is attributed to aliphatic saturated C–H stretching in the glucose units. Additionally, peaks at 1051 cm^{-1} , 1093 cm^{-1} , and 1145 cm^{-1} demonstrate the presence of sulphate ester bonds, which are introduced following the sulphuric acid hydrolysis employed in the CNC preparation.

Mechanical properties of PVA electrospun mats

The mechanical properties of the PVA electrospun mats were obtained from tensile tests and evaluated to qualify their use as wound dressings. The optimum material for dermatological applications needs to be flexible enough to adapt to the structure of the skin, cover the wound to protect it from infection, and possess the necessary mechanical strength to resist external abrasions.^{42,43} Fig. 6 and Table 4 summarise the results from uniaxial tensile tests carried out on the various PVA mats.

Physical cross-linking resulted in a statistically significant increase ($P < 0.05$) in the ultimate tensile strength (UTS) of the mats (6.77 MPa *c.f.* 3.46 MPa for the untreated ones) and a statistically significant decrease in the elongation at break (30.0 *c.f.* 54.2 for the untreated ones). This is an expected result, since the annealing process increases the degree of crystallinity (shown in Fig. 7 and the corresponding text) due to the exposure at high temperatures, which reduces the chain mobility in the polymeric network and creates stiffer mats compared to the more amorphous untreated PVA polymer.^{44,45} Chemical-linking also increased the tensile strength of the materials compared to the control, with a statistically significant increase in the UTS for PVA (1), PVA(2), PVA(3), and PVA(4) as compared to PVA(C). The same trend was seen with the Young's Moduli of the samples, with a statistically significant difference being found between all samples containing cross-linker as compared to the control PVA(C).

However, there was no direct correlation between the amount of cross-linker and the UTS, even though there was a significant decrease in Young's Modulus seen between PVA(1) and PVA(4), but not between PVA(H) and PVA(4).

The elongation at break increased with decreasing citric acid and glyoxal content, producing tougher mats^{46,47} with a statistically significant difference between PVA(1), the sample with the highest percentage of cross-linker, and all other samples — aside from the physically cross-linked sample PVA(H).

The outstanding mechanical properties of cellulose are well documented,^{27,34,48} and as expected, the addition of cellulose nanocrystals (CNC) increased the Young's modulus and the tensile strength compared to PVA(1), which contains the same concentration of cross-linking agents. By increasing the concentration of CNC in the polymer, stronger mats were produced but the elongation at break was not altered. Strong interfacial interactions between PVA and CNC by intermolecular hydrogen bonding contribute to the reinforcement of the mechanical properties in the PVA-loading mats.

Degree of crystallinity

The degree of crystallinity was found to depend both on the heat treatment and on the presence of cross-linkers in the samples. The non-thermally treated samples (Fig. 7) displayed relatively broad reflections at $\sim 2\theta = 19.4^\circ$ and $\sim 2\theta = 40.8^\circ$, which correspond to the (101) and (220) phases of semi-crystalline PVA, respectively. Annealing the samples to 125°C leads to narrowing of both of these reflections, along with the appearance of a sharp reflection at $2\theta = 22.4^\circ$ corresponding to the crystalline (200) phase of PVA cross-linked fibers.⁴⁹ Furthermore, the crystallinity following heat treatment was found to increase with increasing amounts of cross-linkers present in the sample, with PVA(1) showing more intense and narrower reflections as compared to PVA(4). It is worth noting that the PVA(H) sample, which was physically cross-linked by heating at 180°C , presented the same reflections as the chemically cross-linked samples, suggesting a thermally-induced increase in crystallinity (thermal annealing).

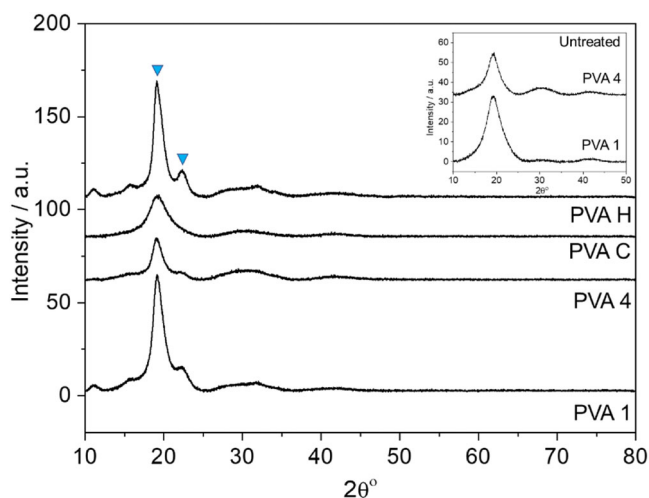


Figure 7. XRD patterns of the thermally treated PVA(1) and PVA(4) samples as well as PVA(H) and PVA(C). The two inverted blue triangles indicate 2θ values of 19.4° and 22.4° . The inset shows the corresponding diffractograms of PVA(1) and PVA(4) before thermal treatment.

Dissolution profiles of PVA electrospun mats

Controllable degradability is an important property of the electrospun mats, and this feature provides them with the flexibility to be used for different biomedical applications, from wound healing to drug delivery and tissue engineering.^{35,50-52} The dissolution profiles of the non-woven PVA materials were investigated and the results are presented in Fig. 8. The data corroborate that cross-linking improved the water resistance of the mats. Untreated mats rapidly dissolved in water due to their high surface area and the enhanced water solubility of the PVA polymer;⁵³ on the other hand, following physical and chemical cross-linking, weight loss took place mostly during the first 24 h and was higher for the specimens with lower concentrations of glyoxal and citric acid. After 6 days in water, PVA(1), which was prepared with 1% (w/w) citric acid and 0.5% (w/w) glyoxal, exhibited $<2\%$ weight loss only, while the heat-treated PVA(H) lost 24% of its initial weight, confirming that chemical cross-linking of the polymer chains inhibits water transport through the polymer network.⁵⁴ Furthermore, our data demonstrate that the degradation profile of the chemically cross-linked PVA can be controlled by varying the concentrations of CA and glyoxal cross-linking agents.⁵⁵ The physically cross-linked sample PVA(H) had relatively rapid weight loss compared to the rest of the samples (Fig. 8). Mirafteb and co-workers⁴⁴ explored the effect of heat treatment on PVA electrospun mats and demonstrated that no weight loss occurred when high molecular weight PVA (146–186 kDa, 99% hydrolysed) mats, which were heat treated at 180°C for 30 min, were immersed in water for 24 h at room temperature. This discrepancy with our results is attributed to the differences in the degree of hydrolysis between the samples (88% for our PVA) which affects water solubility, ability to crystallize, mechanical properties, and water resistance (all being higher for higher degrees of hydrolysis).²²

Adding the cellulose nanocrystals did not appear to have an impact on the dissolution of the PVA mats and, following water immersion for 6 days, the weight loss remained similar (1.58% for PVA(1)/CNC(1) and 2.08% for PVA(1)/CNC(2)) to that of the PVA without any additives (1.96% for PVA(1)).

Cytotoxicity of PVA electrospun mats

The biocompatibility of the cross-linked mats was studied by exposing them to cultures of human fibroblasts cells. Dermal

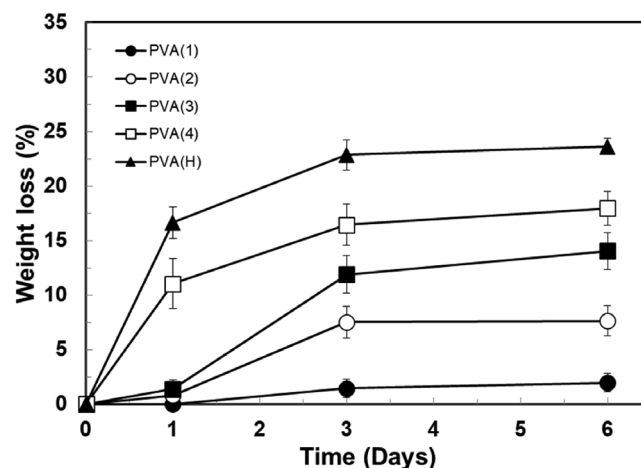


Figure 8. Weight loss of PVA mats following immersion in DI water at room temperature.

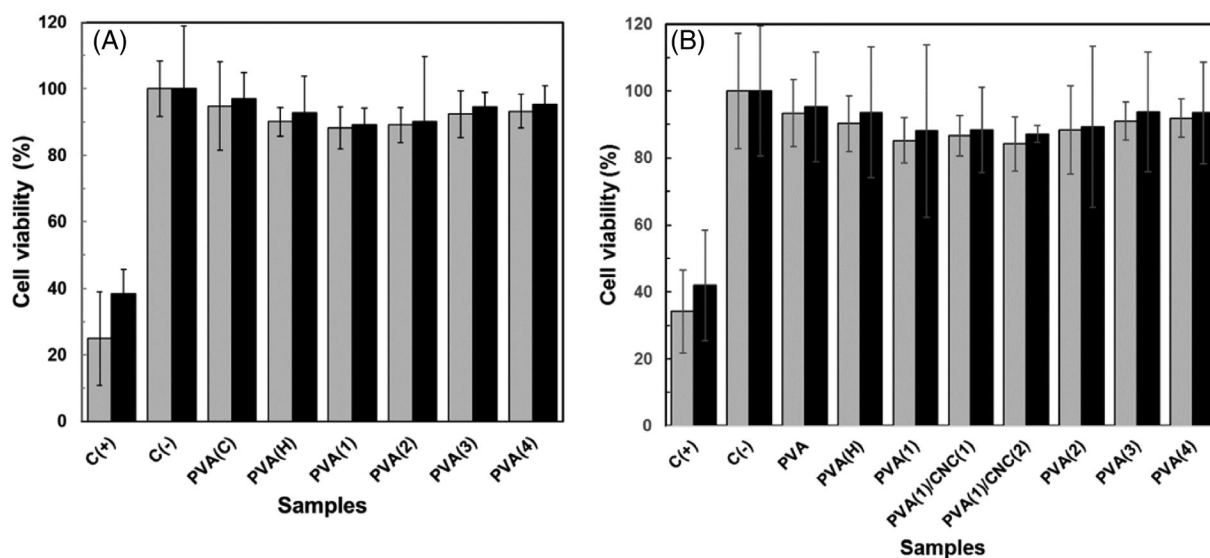


Figure 9. Cell metabolic activity of human fibroblasts after exposure to PVA electrospun mats (A = indirect test; B = direct test) for 24 h (grey bars) and 72 h (black bars). C (+) refers to the cytotoxic response in the presence of 70% (v/v) ethanol, and C (–) corresponds to cell growth in the absence of mats (n = 5 for CNC mats; n = 6 in all other cases).

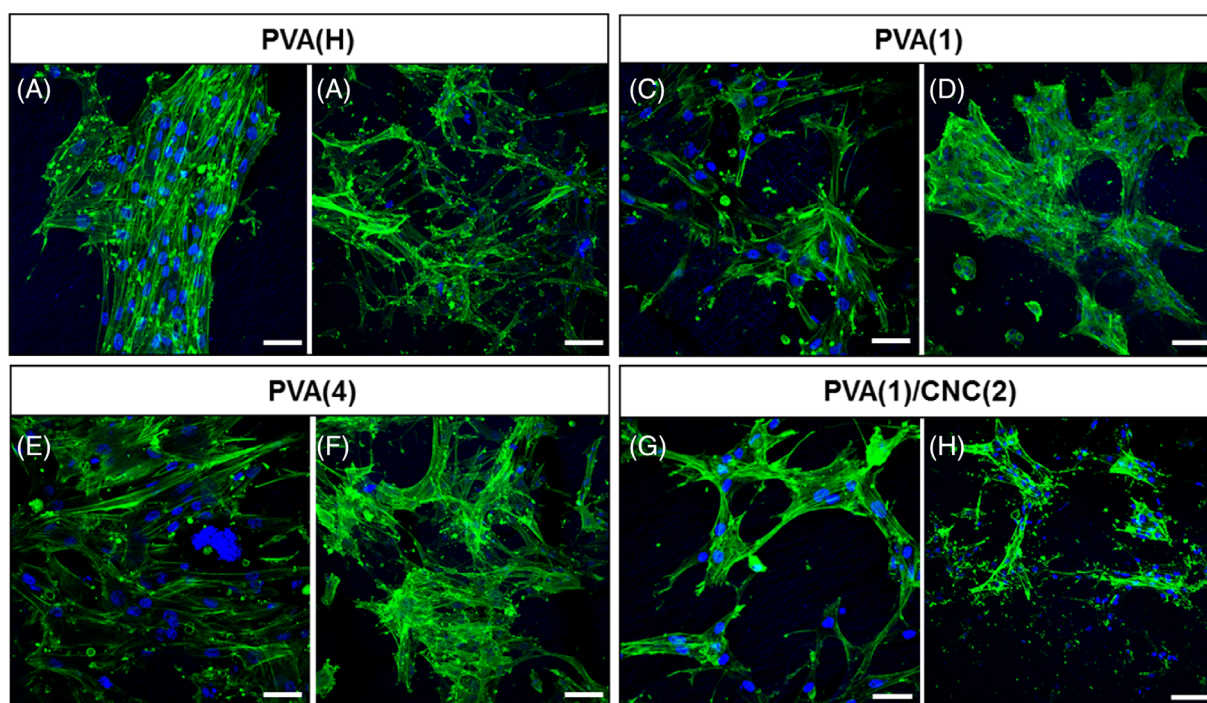


Figure 10. Fluorescent microscope images of nucleus (Hoechst, blue) and Actin filaments (GreenActin, green) staining of 142BR fibroblasts after 24 h (A, C, E, G) and 72 h (B, D, F, H) contact with PVA electrospun mats. Cells were observed whilst fully attached to the material. Scale bars: 50 μ m (A, C, E, G); 100 μ m (B, D, F, H).

fibroblasts play a crucial role in wound healing because they contribute to the production of the extracellular matrix formation that regenerates the skin structure.^{56,57} Cytotoxicity tests were carried out according to the standard condition methods of ISO 10993-5, which mimic the physiological conditions of the human body. For the scaffold materials to be used as a supporting platform for cell growth and proliferation, it is important that they maintain their structure when in contact with an aqueous medium and that they

have no cytotoxic effect due to the reagents used to create permanent and stable linkages between the polymer chains.^{58,59}

Recently, it has been shown that carboxylic acids can be used to cross-link biomaterials without compromising their cytocompatibility.⁶⁰ Citric acid is a metabolic product in the Krebs cycle and, therefore, an endogenous intermediate of the body, which makes it suitable for biomedical applications.^{61–63} In the case of PVA, however, concentrations of >20% (based on polymer weight) of

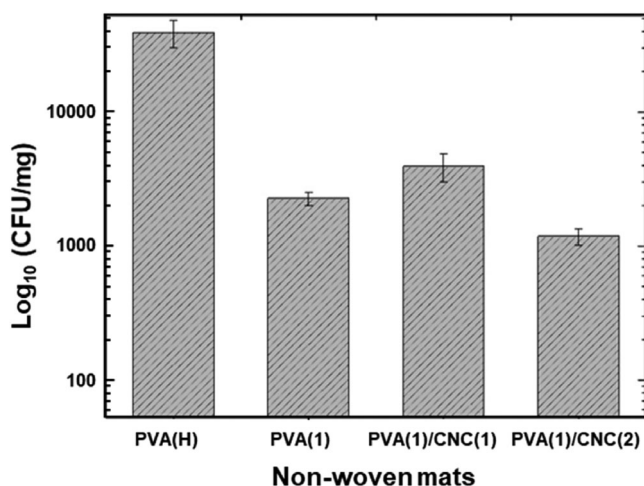


Figure 11. Colony-forming units (CFU) for *S. aureus* following detachment from the surface of the PVA mats after exposure to an initial bacterial culture of 10^6 cells/mL over a 24 h period at 36 °C.

citric acid are required to achieve good water stability.⁶⁴ The use of aldehydes, on the other hand, could be controversial due to their toxicity profile. Glutaraldehyde has been used extensively as a cross-linking agent despite the fact that it can produce a toxic effect, even at low concentrations.⁶⁵ As a promising alternative, this work evaluates the use of glyoxal, a smaller dialdehyde with the advantage of being readily biodegradable and less toxic than similar reagents.^{41,66} Glyoxal is endogenously produced during the normal cellular metabolism and is present in human blood plasma (at concentrations 0.1–1 $\mu\text{mol L}^{-1}$) and in fermented food and beverages.^{67–70} It is an important intermediate in the formation of advanced glycation end-products (AGEs), which disturb cellular metabolism, impair proteolysis, and inhibit cell

proliferation and protein synthesis; however, its deleterious effects are counteracted by the glyoxalase system, which converts glyoxal to the less-reactive glycolate.⁷⁰ Data on the effect of glyoxal in humans is limited, but there are very few indications of contact sensitization in the presence of at least 10% glyoxal during long-term exposure,^{70,71} along with some decrease in cell viability at high concentrations.^{23,72} Therefore, in this study, very low concentrations ($\leq 0.5\%$ w/w) of glyoxal were selected to ensure cytocompatibility.

The potential cytotoxicity of the electrosun mats was assessed using human fibroblast cells (134BR) after 24 and 72 h of contact. Both the extract test (Fig. 9(A)), which looks into the effect of leachable entities from the dissolution of the PVA mats, and the direct test (Fig. 9(B)), which analyses the effects of physical cell-surface interaction, showed a small decrease (of up to 8% compared to PVA(C)) in cell viability with increased glyoxal concentration. Physically cross-linked mats (PVA(H)) and those produced using 0.06% and 0.12% (w/w) glyoxal (PVA(4) and PVA(3), respectively) showed the lowest reduction in their biocompatibility, which ranged between 2% and 4% compared to the non-cross-linked mats. Shangari and O'Brien explored the cytotoxic mechanism of glyoxal using rat hepatocytes and concluded that, above 5 mmol L^{-1} , it can induce the collapse of mitochondrial membrane potential and also lipid peroxidation and formaldehyde formation.⁶⁸ Wang and Stegemann,²³ on the other hand, found that up to 100 mmol L^{-1} of glyoxal cross-linker in the preparation of their chitosan/collagen hydrogel matrices had no effect on the viability of human bone marrow stem cells after 1 h exposure, but for longer periods (up to 9 days), cells remained >90% viable at a reduced glyoxal concentration of 1 mmol L^{-1} . Similarly, Koosha and co-workers⁷³ demonstrated excellent fibroblast biocompatibility, even after 15 days of cell culture, using their chitosan/PVA nanofibers cross-linked 5% (v/v) glyoxal.

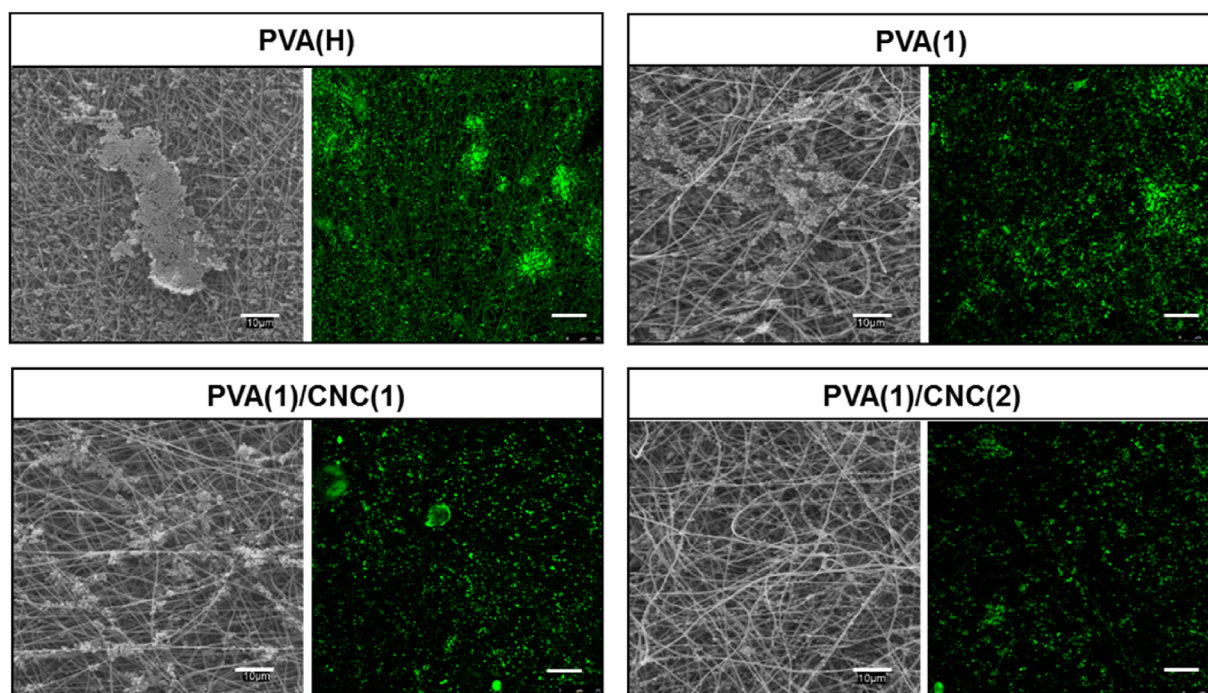


Figure 12. SEM and FilmTracer FM-43 Green Biofilm Cell Stain confocal micrographs of the surface of the mats exposed to *S. aureus* cultures at 36 °C for 24 h. Scale bars: 10 μm (SEM images); 20 μm (Confocal images).

Fluorescence imaging was used to confirm the MTT assay results. Figure 10 shows confocal images of PVA(H), PVA(1), PVA(1)/CNC(2), and PVA(4) scaffolds that were kept in contact with human fibroblast cells for 24 and 72 h. The images for the rest of the specimens with different concentrations of cross-linking agents (PVA(2) and PVA(3)) and lower concentration of cellulose nanocrystals (PVA(1)/CNC(1)) are shown in Fig. S5. The cluster of cells over the scaffold surface indicates cell proliferation, whereas F-actin filaments confirm that the cells conserved their characteristic elongated morphology after contact with the PVA surfaces.

Cell proliferation was also visualised using optical microscopy (Fig. S6) and the spreading of cells after being in contact with the mats for 72 h further confirmed the biocompatibility of the PVA supports. An interesting point to note is that the areas of the mats not covered with cells appeared to maintain their nanofibrous structure, and this further validates the effectiveness of the cross-linking method employed in this study.

Antimicrobial behaviour of PVA electrospun mats

The 'ideal' dressing should protect the wound from infection and, therefore, antimicrobial properties are highly desirable. The antibacterial activity of the mats containing the highest amount of cross-linking agents, with and without cellulose nanocrystals (CNC), was evaluated against the growth of *Staphylococcus aureus* (*S. aureus*), a gram-positive bacterium responsible for major skin and soft-tissue infections in humans.^{74,75} As shown in Fig. 11, there is a significant antimicrobial effect (>1 log bacterial reduction) for all mats containing the highest concentration of the cross-linking agents compared to the 'neat' PVA mats, which have undergone just physical cross-linking using heat treatment (PVA(H)). The glyoxal used to cross-link the PVA mats seemed to have some antibacterial efficacy. Although the exact mechanism is not known in detail, some research suggests that, due to its similar chemical structure to other aldehydes (such as formaldehyde and glutaraldehyde), glyoxal could interact directly with bacterial proteins and enzymes, affecting their metabolisms and causing death.^{76,77} Moreover, the CNC incorporation had no influence on the antimicrobial behaviour of these mats, which was expected, since cellulosic materials do not intrinsically present antibacterial and/or antimicrobial properties.³⁴ It is worth noting, however, that the high surface area and hydroxyl groups of CNC offer the opportunity for chemical modification and incorporation of different antimicrobial agents, which could improve the antimicrobial efficacy of these mats.^{78,79}

Figure 12 shows SEM micrographs of the surface of the PVA mats whilst in contact with *S. aureus* (initial concentration of 10^6 cells mL^{-1}) for 24 h at 36 °C. A large continuous biofilm appears on the surface of the physically cross-linked PVA(H) mats, whereas the chemically cross-linked ones display certain parts of their surface free from bacteria, with dispersed colonization areas. This was also confirmed by further visualization using FilmTracer FM 1–43. FM 1–43 is a lipophilic dye that binds rapidly and reversibly to the plasma membrane with strong fluorescent enhancement, thereby successfully staining the cells in a complex biofilm milieu. Figure 12 shows that PVA(H) mats exhibited clear and extensive biofilm formation over their surface, unlike their chemically cross-linked counterparts, which appeared considerably cleaner in terms of the biofilm-forming ability of *S. aureus* over their surface.

CONCLUSIONS

Continuous, interconnected, and bead-free nanofibers were successfully electrospun from 130 kDa PVA. By varying the mode (physical vs chemical) of cross-linking and the amounts of cross-linkers, and by incorporating nanoparticles in the form of CNC, a series of supports with tailor-made characteristics (in terms of ease of dissolution, swelling properties, and mechanical strength) were created. Increasing the concentration of chemical cross-linkers had a slight deleterious effect on fibroblast viability, but nevertheless, metabolic activity remained above 87% over a 3 day-contact period. The PVA mats cross-linked with 1% (w/w) citric acid and 0.5% (w/w) glyoxal (with and without CNC) revealed a 10-fold reduction in CFU for *S. aureus* (one of the commonest pathogens found in wound infections) and there was a lack of extended biofilm formation compared to the physically cross-linked (heat-treated) mats.

ACKNOWLEDGEMENTS

Financial support for this work was provided by the Dirección General de Universidades e Investigación de la Comunidad de Madrid Research Network S2013/MAE-2716. BD would like to acknowledge the University of Alcalá for the pre-doctoral grant award.

SUPPORTING INFORMATION

Supporting information may be found in the online version of this article.

REFERENCES

- Caló E and Khutoryanskiy VV, Biomedical applications of hydrogels: a review of patents and commercial products. *Eur Polym J* **65**:252–267 (2015).
- Fu Q, Duan C, Yan Z, Li Y, Liu L, Yu J *et al.*, Nanofiber-based hydrogels: controllable synthesis and multifunctional applications. *Macromol Rapid Commun* **39**:1800058 (2018).
- Shankhwar N, Kumar M, Mandal BB, Robi PS and Srinivasan A, Electrospun poly(vinyl alcohol)-poly(vinyl pyrrolidone) nanofibrous membranes for interactive wound dressing application. *Aust J Biol Sci* **27**:247–262 (2016).
- Jannesari M, Varshosaz J, Morshed M and Zamani M, Composite poly(vinyl alcohol)/poly(vinyl acetate) electrospun nanofibrous mats as a novel wound dressing matrix for controlled release of drugs. *Int J Nanomedicine* **6**:993–1003 (2011).
- Sundaramurthi D, Krishnan UM and Sethuraman S, Electrospun nanofibers as scaffolds for skin tissue engineering. *Polym Rev* **54**:348–376 (2014).
- Aliko K, Aldakhalla MB, Leslie LJ, Worthington T, Topham PD and Theodosiou E, Poly(butylene succinate) fibrous dressings containing natural antimicrobial agents. *J Ind Text* (2021). <https://doi.org/10.1177/1528083720987209>
- Alenezi MH, Cam ME and Edirisinghe M, Experimental and theoretical investigation of the fluid behaviour during polymeric fiber formation with and without pressure. *Appl Phys Rev* **6**:041401 (2019).
- Jia Y, Yang C, Chen X, Xue W, Hutchins-Crawford HJ, Yu Q *et al.*, A review on electrospun magnetic nanomaterials: methods, properties and applications. *J Mater Chem C* **9**:9042–9082 (2021). <https://doi.org/10.1039/D1TC01477C>
- Hassiba AJ, El Zowalaty ME, Webster TJ, Abdullah AM, Nasrallah GK, Khalil KA *et al.*, Synthesis, characterization, and antimicrobial properties of novel double layer nanocomposite electrospun fibers for wound dressing applications. *Int J Nanomedicine* **12**:2205–2213 (2017).
- Chen L, Wang S, Yu Q, Topham PD, Chen C and Wang L, A comprehensive review of electrospinning block copolymers. *Soft Matter* **15**:2490–2510 (2019).

- 11 Kumkun P, Tuancharoensri N, Ross G, Mahasaron S, Jongjitwimol J, Topham PD *et al.*, Green fabrication route of robust, biodegradable silk sericin and poly(vinyl alcohol) nanofibrous scaffolds. *Polym Int* **68**:1903–1913 (2019).
- 12 Nkhwa S, Lauriaga KF, Kemal E and Deb S, Poly(vinyl alcohol): physical approaches to designing biomaterials for biomedical applications. *Conf Pap Sci* **2014**:1–7 (2014).
- 13 Akhtar MF, Hanif M and Ranjha NM, Methods of synthesis of hydrogels. A review. *Saudi Pharm J* **24**:554–559 (2016).
- 14 Hennink WE and van Nostrum CF, Novel cross-linking methods to design hydrogels. *Adv Drug Deliv Rev* **54**:13–36 (2002).
- 15 Parhi R, Cross-linked hydrogel for pharmaceutical applications: a review. *Adv Pharm Bull* **7**:515–530 (2017).
- 16 Oryan A, Kamali A, Moshiri A, Baharvand H and Daemi H, Chemical cross-linking of biopolymeric scaffolds: current knowledge and future directions of crosslinked engineered bone scaffolds. *Int J Biol Macromol* **107**:678–688 (2018).
- 17 Ratanavaraporn J, Rangkupan R, Jeeratawatchai H, Kanokpanont S and Damrongsakul S, Influences of physical and chemical cross-linking techniques on electrospun type a and B gelatin fiber mats. *Int J Biol Macromol* **47**:431–438 (2010).
- 18 Jingjing Shi EY, Green electrospinning and cross-linking of polyvinyl alcohol/ citric acid. *J NanoR* **32**:32–42 (2015).
- 19 Jose J and Al-Harhi MA, Citric acid cross-linking of poly(vinyl alcohol)/starch/graphene nanocomposites for superior properties. *Iran Polym J* **26**:579–587 (2017).
- 20 Zhang Y, Zhu PC and Edgren D, Cross-linking reaction of poly(vinyl alcohol) with glyoxal. *J Polym Res* **17**:725–730 (2010).
- 21 Çay A, Akçakoca Kumbasar EP, Keskin Z, Akduman Ç and Şendemir Ürkmez A, Cross-linking of poly(vinyl alcohol) nanofibres with polycarboxylic acids: biocompatibility with human skin keratinocyte cells. *J Mater Sci* **52**:12098–12108 (2017).
- 22 Park JY, Hwang KJ, Yoon SD, Lee JH and Lee IH, Influence of Glyoxal on preparation of poly(vinyl alcohol)/poly(acrylic acid) blend film. *J Nanosci Nanotechnol* **15**:5955–5958 (2015).
- 23 Wang L and Stegemann JP, Glyoxal cross-linking of cell-seeded chitosan/collagen hydrogels for bone regeneration. *Acta Biomater* **7**:2410–2417 (2011).
- 24 Rieger KA, Birch NP and Schiffman JD, Designing electrospun nanofiber mats to promote wound healing – a review. *J Mater Chem B* **1**:4531–4541 (2013).
- 25 Simões D, Miguel SP, Ribeiro MP, Coutinho P, Mendonça AG and Correia IJ, Recent advances on antimicrobial wound dressing: a review. *Eur J Pharm Biopharm* **127**:130–141 (2018).
- 26 Chakrabarty A and Teramoto Y, Recent advances in nanocellulose composites with polymers: a guide for choosing partners and how to incorporate them. *Polymers* **10**:517 (2018).
- 27 Trache D, Tarchoun AF, Derradji M, Hamidon TS, Masruchin N, Brosse N *et al.*, Nanocellulose: from fundamentals to advanced applications. *Front Chem* **8**:392 (2020).
- 28 Ghafari R, Scaffaro R, Maio A, Gulino EF, Lo Re G and Jonoobi M, Processing-structure-property relationships of electrospun PLA-PEO membranes reinforced with enzymatic cellulose nanofibers. *Polym Test* **81**:106182 (2020).
- 29 ISO standard 10993-5:2009, Biological evaluation of medical devices - Part 5: Tests for in vitro cytotoxicity. 3rd Edition (2009). Accessed 1st December 2021.
- 30 Wang MO, Etheridge JM, Thompson JA, Vorwald CE, Dean D and Fisher JP, Evaluation of the in vitro cytotoxicity of cross-linked biomaterials. *Biomacromolecules* **14**:1321–1329 (2013).
- 31 Swain SK and Sarkar D, Fabrication, bioactivity, in vitro cytotoxicity and cell viability of cryo-treated nanohydroxyapatite–gelatin–polyvinyl alcohol macroporous scaffold. *J Asian Ceramic Soc* **2**:241–247 (2014).
- 32 Katime I, de Apodaca ED and Rodríguez E, Effect of cross-linking concentration on mechanical and thermodynamic properties in acrylic acid–co–methyl methacrylate hydrogels. *J Appl Polym Sci* **102**:4016–4022 (2006).
- 33 Enayati MS, Behzad T, Sajkiewicz P, Bagheri R, Ghasemi-Mobarakeh L, Łojkowski W *et al.*, Crystallinity study of electrospun poly (vinyl alcohol) nanofibers: effect of electrospinning, filler incorporation, and heat treatment. *Iran Polym J* **25**:647–659 (2016).
- 34 Jorfi M and Foster EJ, Recent advances in nanocellulose for biomedical applications. *J Appl Polym Sci* **132**:app41719 (2015).
- 35 Li W, Yu Q, Yao H, Zhu Y, Topham PD, Yue K *et al.*, Superhydrophobic hierarchical fiber/bead composite membranes for efficient treatment of burns. *Acta Biomater* **92**:60–70 (2019).
- 36 Winter G, Formation of the scab and the rate of Epithelization of superficial wounds in the skin of the young domestic pig. *Nature* **193**:293–294 (1962).
- 37 Field CK and Kerstein MD, Overview of wound healing in a moist environment. *Am J Surg* **167**:S2–S6 (1994).
- 38 Zhang M and Zhao X, Alginate hydrogel dressings for advanced wound management. *Int J Biol Macromol* **162**:1414–1428 (2020).
- 39 Alhosseini SN, Mozarzadeh F, Mozafari M, Asgari S, Dodel M, Samadikuchaksaraei A *et al.*, Synthesis and characterization of electrospun polyvinyl alcohol nanofibrous scaffolds modified by blending with chitosan for neural tissue engineering. *Int J Nanomedicine* **7**:25–34 (2012).
- 40 Meszlényi G and Körtvélyessy G, Direct determination of vinyl acetate content of ethylene-vinyl acetate copolymers in thick films by infrared spectroscopy. *Polym Test* **7**:551–557 (1999).
- 41 Qiu K and Netravali AN, Fabrication and characterization of biodegradable composites based on microfibrillated cellulose and polyvinyl alcohol. *Compos Sci Technol* **72**:1588–1594 (2012).
- 42 MacEwan MR, MacEwan S, Kovacs TR and Batts J, What makes the optimal wound healing material? A review of current science and introduction of a synthetic nanofabricated wound care scaffold. *Cureus* **9**:e1736 (2017).
- 43 Wong RSH, Ashton M and Dodou K, Effect of cross-linking agent concentration on the properties of unmediated hydrogels. *Pharmaceutics* **7**:305–319 (2015).
- 44 Mirafteb M, Saifullah A and Çay A, Physical stabilisation of electrospun poly(vinyl alcohol) nanofibres: comparative study on methanol and heat-based crosslinking. *J Mater Sci* **50**:1943–1957 (2015).
- 45 Wong KKH, Zinke-Allmag M and Wan W, Effect of annealing on aqueous stability and elastic modulus of electrospun poly(vinyl alcohol) fibers. *J Mater Sci* **45**:2456–2465 (2010).
- 46 Cui Z, Zheng Z, Lin L, Si J, Wang Q, Peng X *et al.*, Electrospinning and cross-linking of polyvinyl alcohol/chitosan composite nanofiber for transdermal drug delivery. *Adv Polym Technol* **37**:1917–1928 (2016).
- 47 Rudra R, Kumar V and Kundu PP, Acid catalysed cross-linking of poly vinyl alcohol (PVA) by glutaraldehyde: effect of crosslink density on the characteristics of PVA membranes used in single chambered microbial fuel cells. *RSC Adv* **5**:83436–83447 (2015).
- 48 Tarrés Q, Oliver-Ortega H, Alcalà M, Espinach FX, Mutjé P and Delgado-Aguilar M, Research on the strengthening advantages on using cellulose nanofibers as polyvinyl alcohol reinforcement. *Polymers* **12**:974 (2020).
- 49 Roy S, Kuddannaya S, Das T, Lee HY, Lim J, Hu XM *et al.*, A novel approach for fabricating highly tunable and fluffy bioinspired 3D poly(vinyl alcohol) (PVA) fiber scaffolds. *Nanoscale* **9**:7081–7093 (2017).
- 50 Liu M, Duan X-P, Li Y-M, Yang D-P and Long Y-Z, Electrospun nanofibers for wound healing. *Mater Sci Eng C* **76**:1413–1423 (2017).
- 51 Tuancharoensri N, Ross GM, Mahasaron S, Topham PD and Ross S, Ternary blend nanofibres of poly (lactic acid), polycaprolactone and cellulose acetate butyrate for skin tissue scaffolds: influence of blend ratio and polycaprolactone molecular mass on miscibility, morphology, crystallinity and thermal properties. *Polym Int* **66**:1463–1472 (2017).
- 52 Wang L, Wang M, Topham PD and Huang Y, Fabrication of magnetic drug-loaded polymeric composite nanofibres and their drug release characteristics. *RSC Adv* **2**:2433–2438 (2012).
- 53 Lopez-Cordoba A, Castro GR and Goyanes S, A simple green route to obtain poly(vinyl alcohol) electrospun mats with improved water stability for use as potential carriers of drugs. *Korean J Couns Psychother* **69**:726–732 (2016).
- 54 Mallapragada SK and Peppas NA, Dissolution mechanism of semicrystalline poly(vinyl alcohol) in water. *J Polym Sci B* **34**:1339–1346 (1996).
- 55 Sonker AK, Rathore K, Nagarale RK and Verma V, Cross-linking of polyvinyl alcohol (PVA) and effect of crosslinker shape (aliphatic and aromatic) thereof. *J Polym Environ* **26**:1782–1794 (2018).
- 56 Tracy LE, Minasian RA and Catterson EJ, Extracellular matrix and dermal fibroblast function in the healing wound. *Adv Wound Care* **5**:119–136 (2016).
- 57 Nilforoushzadeh MA, Ahmadi Ashtiani HR, Jaffary F, Jahangiri F, Nikkiah N, Mahmoudbeyk M *et al.*, Dermal fibroblast cells: biology and function in skin regeneration. *J Skin Stem Cell* **4**:e69080 (2017).

- 58 Azmi S, Abd Razak SI, Kadir MRA, Iqbal N, Hassan R, Nayan NHM *et al.*, Reinforcement of poly(vinyl alcohol) hydrogel with halloysite nanotubes as potential biomedical materials. *Soft Mater* **15**:45–54 (2017).
- 59 Fideles TB, Santos JL, Thomás H, Furtadi GTFS, Lima DB, Borges SMP *et al.*, Characterization of chitosan membranes Crosslinked by sulfuric acid. *OALib J* **5**:e4336 (2018).
- 60 Reddy N, Reddy R and Jiang Q, Cross-linking biopolymers for biomedical applications. *Trends Biotechnol* **33**:362–369 (2015).
- 61 Shi R, Bi J, Zhang Z, Zhu A, Chen D, Zhou X *et al.*, The effect of citric acid on the structural properties and cytotoxicity of the polyvinyl alcohol/starch films when molding at high temperature. *Carbohydr Polym* **74**:763–770 (2008).
- 62 Gyawali D, Nair P, Zhang Y, Tran RT, Zhang C, Samchukov M *et al.*, Citric acid-derived in situ crosslinkable biodegradable polymers for cell delivery. *Biomaterials* **31**:9092–9105 (2010).
- 63 Tran RT, Yang J and Ameer GA, Citrate-based biomaterials and their applications in regenerative engineering. *Annu Rev Mat Res* **45**: 277–310 (2015).
- 64 Truong YB, Choi J, Mardel J, Gao Y, Maisch S, Musameh M *et al.*, Functional cross-linked electrospun polyvinyl alcohol membranes and their potential applications. *Macromol Mater Eng* **302**:1700024 (2017).
- 65 Barkay-Olami H and Zilberman M, Novel porous soy protein-based blend structures for biomedical applications: microstructure, mechanical, and physical properties. *J Biomed Mater Res B Appl Biomater* **104**:1109–1120 (2016).
- 66 Heo GS, Cho S and Wooley KL, Aldehyde-functional polycarbonates as reactive platforms. *Polym Chem* **5**:3555–3558 (2014).
- 67 Kasper M, Roehlecke C, Witt M, Fehrenbach H, Hofer A, Miyata T *et al.*, Induction of apoptosis by glyoxal in human embryonic lung epithelial cell line L132. *Am J Respir Cell Mol Biol* **23**:485–491 (2000).
- 68 Shangari N and O'Brien PJ, The cytotoxic mechanism of glyoxal involves oxidative stress. *Biochem Pharmacol* **68**:1433–1442 (2004).
- 69 Thornalley PJ, Glutathione-dependent detoxification of alpha-oxoaldehydes by the glyoxalase system: involvement in disease mechanisms and antiproliferative activity of glyoxalase I inhibitors. *Chem Biol Interact* **111–112**:137–151 (1998).
- 70 Kielhorn J, Pohlenz-Michel C, Schmidt S and Mangelsdorf I, Concise International Chemical Assessment Document 57 – Glyoxal. World Health Organization (2004). <https://apps.who.int/iris/handle/10665/42867>. Accessed 1st December 2021.
- 71 European Commission Health and Consumer Protection Directorate-General, Scientific committee on consumer products opinion on Glyoxal. C7 Risk Assessment SCCP/0881/05 (2005). Accessed 1st December 2021.
- 72 Suwantong O, Pavasant P and Supaphol P, Electrospun Zein fibrous membranes using Glyoxal as cross-linking agent: preparation, characterization and potential for use in biomedical applications. *Chiang Mai J Sci* **38**:56–70 (2011).
- 73 Koosha M, Raoufi M and Moravvej H, One-pot reactive electrospinning of chitosan/PVA hydrogel nanofibers reinforced by halloysite nanotubes with enhanced fibroblast cell attachment for skin tissue regeneration. *Colloid Surf B Biointerf* **179**:270–279 (2019).
- 74 Zhang LJ, Guerrero-Juarez CF, Hata T, Bapat SP, Ramos R, Plikus MV *et al.*, Innate immunity. Dermal adipocytes protect against invasive *Staphylococcus aureus* skin infection. *Science* **347**:67–71 (2015).
- 75 Cho JS, Pietras EM, Garcia NC, Ramos RI, Farzam DM, Monroe HR *et al.*, IL-17 is essential for host defense against cutaneous *Staphylococcus aureus* infection in mice. *J Clin Invest* **120**:1762–1773 (2010).
- 76 Kittinaovarat S, Kantuptim P and Singhaboonponp T, Wrinkle resistant properties and antibacterial efficacy of cotton fabrics treated with glyoxal system and with combination of glyoxal and chitosan system. *J Appl Polym Sci* **100**:1372–1377 (2006).
- 77 Jiang L, Li M, Tang J, Zhao X, Zhang J, Zhu H *et al.*, Effect of different disinfectants on bacterial aerosol diversity in poultry houses. *Front Microbiol* **9**:2113 (2018).
- 78 Bepalova Y, Kwon D and Vasanthan, surface modification and antimicrobial properties of cellulose nanocrystals. *J Appl Polym Sci* **134**: 44789 (2017).
- 79 Tavakolian M, Okshevsky M, van de Ven TGM and Tufenkji N, Developing antibacterial nanocrystalline cellulose using natural antibacterial agents. *ACS Appl Mater Interfaces* **10**:33827–33838 (2018).